Thyroid Hormone Insufficiency during Brain Development Reduces Parvalbumin Immunoreactivity and Inhibitory Function in the Hippocampus

M. E. Gilbert, L. Sui, M. J. Walker, W. Anderson, S. Thomas, S. N. Smoller, J. P. Schon, S. Phani, and J. H. Goodman

Neurotoxicology Division (M.E.G., L.S., W.A.), U.S. Environmental Protection Agency, Research Triangle Park, North Carolina 27711; Department of Psychology (M.E.G.), University of North Carolina, Chapel Hill, North Carolina 27599; National Research Council (L.S.), Washington, D.C. 20001; and Center for Neural Recovery and Rehabilitation Research (M.J.W., S.T., S.N.S., J.P.S., S.P., J.H.G.), Helen Hayes Hospital, West Haverstraw, New York 10993

Thyroid hormones are necessary for brain development. γ-Amino-butyric acid (GABA)ergic interneurons comprise the bulk of local inhibitory circuitry in brain, many of which contain the calcium binding protein, parvalbumin (PV). A previous report indicated that severe postnatal hypothyroidism reduces PV immunoreactivity (IR) in rat neocortex. We examined PV-IR and GABA-mediated synaptic inhibition in the hippocampus of rats deprived of thyroid hormone from gestational d 6 until weaning on postnatal d 30. Pregnant dams were exposed to propylthiouracil (0, 3, 10 ppm) via the drinking water, which decreased maternal serum T_4 by approximately 50–75% and increased TSH. At weaning, T_4 was reduced by approximately 70% in offspring in the low-dose group and fell below detectable levels in high-dose animals. PV-IR was diminished in the hippocampus and neocortex of offspring killed on postnatal d 21, an effect that could be reversed by postnatal administration of T_4. Dose-dependent decreases in the density of PV-IR neurons were observed in neocortex and hippocampus, with the dentate gyrus showing the most severe reductions (50–75% below control counts). Altered staining persisted to adulthood despite the return of thyroid hormones to control levels. Developmental cross-fostering and adult-onset deprivation studies revealed that early postnatal hormone insufficiency was required for an alteration in PV-IR. Synaptic inhibition of the perforant path-dentate gyrus synapse evaluated in adult offspring, *in vivo*, revealed dose-dependent reductions in paired pulse depression indicative of a suppression of GABA-mediated inhibition. These data demonstrate that moderate degrees of thyroid hormone insufficiency during the early postnatal period permanently alters interneuron expression of PV and compromises inhibitory function in the hippocampus. (*Endocrinology* 148: 92–102, 2007)

I T IS WELL ESTABLISHED that thyroid hormones are necessary for normal brain development. Severe hormone deprivation leads to reductions in physical growth and mental retardation, particularly if insufficiency occurs in the early postnatal period (1–3). Traditionally animal studies examining the effect of thyroid hormones on brain development were designed to mimic extreme conditions of hormone deprivation (2, 3). In light of mounting evidence that subtle impairments in cognitive abilities accompany mild and circumscribed periods of hormone insufficiency, recent studies have begun to examine the dose-response characteristics of thyroid hormone disruption on brain development (4–7). In addition, significant attention has now focused on not only evaluating the persistence of effects mediated by early hormone insufficiencies but also including an analysis of the functional consequences induced by such perturbations (5, 8, 9).

Disruptions in excitatory synaptic transmission in hippocampus in rats after *in utero* and early postnatal thyroid hormone insufficiency have been reported (10–13). Impairments evident in cornu ammonis (CA1) and dentate subregions of the hippocampal formation endured to adulthood despite return of hormonal status to control levels. In adult assessments of hippocampal long-term potentiation, a cellular model of memory, impairments evident in dendritic recording sites, were accompanied by a curious increase in indices of somatic output as measured by the population spike, suggestive of altered inhibitory function (5, 14–16).

Somatic output of cortical networks is modulated by local circuit interneurons, the majority of which have γ-amino-butyric acid (GABA) as their neurotransmitter (17–20). A subset of inhibitory interneurons also synthesize the calcium binding protein, parvalbumin (PV). PV confers on the interneuron specific electrical and metabolic properties that can impact their function (17–22). PV-expressing interneurons are basket cells and chandelier cells that synapse directly on the soma or initial axonal segment of principal cells of hippocampus and neocortex. Activation of these local circuit neurons effectively limits the firing of action potentials by pyramidal cells of the cortex and hippocampus and granule cells of the dentate gyrus (18–20, 23). Previous work identified a decrease in PV immunoreactivity (IR) in the neocortex of adult hypothyroid animals exposed to a hormone

synthesis inhibitor throughout life and thyroidectomized shortly after birth to produce a persistent and severe state of hypothyroidism (24). Recently reductions in PV-IR have been also reported in the hippocampus of mice with mutations of the TRα1 gene (9, 25). We sought to determine whether severe hormone deprivation was necessary for altered PV-IR or whether modest reductions during critical developmental windows were sufficient. We describe a reduction in PV-IR in cortex similar to that reported by Berbel *et al.* (24) and extend these observations to the cortex and hippocampus of animals with moderate degrees of hormone insufficiency. Importantly, although some recovery ensued on termination of exposure and return to euthyroid status in adulthood, significant suppression of PV-IR remained. These persistent alterations in PV-IR in hippocampal interneurons were associated with functional deficits in inhibitory synaptic transmission in the dentate gyrus.

Materials and Methods

Subjects

Pregnant Long-Evans rats were obtained from Charles River (Raleigh, NC) on gestational day (GD) 2 and housed individually in standard plastic hanging cages in an Association for Assessment and Accreditation of Laboratory Animal Care-approved animal facility. All animal treatments were in strict accordance with the National Institutes of Health Guide for the Care and Use of Laboratory Animals. All efforts were made to minimize the number of animals and their suffering. Animal rooms were maintained on a 12-h light, 12-h dark schedule, and animals were permitted free access to food (rat chow; Purina, St. Louis, MO) and water.

Hormone insufficiency during development

Beginning on GD 6 and continuing until postnatal day (PN) 30, dams were rendered hypothyroid by addition of 0, 3, or 10 ppm (0, 18, or 59 μM solutions, respectively) of the thyroid hormone synthesis inhibitor propylthiouracil (PTU; Sigma, St. Louis, MO) to the drinking water. The day of birth was designated PN0 and all litters were culled to 10 pups on PN4, retaining the maximal number of males per litter. On PN30, the offspring were weaned, transferred to plastic hanging cages (two to four/cage) and were permitted free access to food and tap water. A subset of animals (one per litter) was killed on PN14, PN21, and PN77 for Western blot analysis. A second series of pups was killed on PN23 and PN86 and processed for immunohistochemical assessment of PV staining in cortex and hippocampus. A third set of littermates was prepared for electrophysiological assessment of inhibitory function in the dentate gyrus as described below. These conditions produced graded levels of thyroid hormone reduction in dams and pups as previously reported in Sui *et al.* (16), and serum hormones had fully recovered at the time adult animals were killed.

Critical window of exposure

To determine whether a critical window of hormone insufficiency was necessary for altered immunostaining, a cross-fostering study was conducted. Beginning on GD6 and until birth (PN0), 13 dams were placed on 0 ppm (n = 6) or 10 ppm (n = 7) PTU in the drinking water.

On PN1, litters were culled to 10 pups, and half of each litter was tattooed via a sc injection of India ink to the paw of the forelimb and cross-fostered to a dam from the opposite dose group, creating independent groups of pups exposed to one of four *in utero*/postnatal exposure conditions: control/control, prenatal/control, control/postnatal, and prenatal/postnatal. Pups from each condition were killed for immunohistochemistry on PN23.

Thyroid hormone replacement study

Thyroid hormone replacement was accomplished by dosing pups from 10-ppm exposed dams (n = 6) with 100 μg/kg T₄ (Sigma) or saline,

ip, in a volume of 25 μg/ml once daily between PN8 and PN14 corresponding to time window over which PV is first expressed in the cortex and hippocampus (26). Three pups from each litter received saline or T₄. All pups were killed on PN27 via intracardiac perfusion and the brains were prepared for immunohistochemistry.

Adult dosing study

To determine whether hormone insufficiency induced in adult animals could alter PV-IR, a group of 15 naive adult male rats was placed on 0, 3, or 10 ppm PTU in the drinking water for 33 d, beginning on PN56. This duration of PTU exposure was sufficient to produce asymptotic levels of hormone reduction at the specified doses comparable with those achieved in lactating dams at weaning. Animals were killed on the final day of PTU exposure and prepared for immunohistochemistry as described below.

Thyroid hormones

Thyroid hormone data for the developmental study were previously reported by Sui *et al.* (16). In the cross-fostering and adult exposure studies blood was sampled from the heart before saline perfusion and allowed to clot on ice for a minimum of 30 min. Serum was separated via centrifugation and stored at −80 C for later analyses. Serum concentrations of total T₄ and total T₃ were analyzed by RIA (Diagnostic Products Corp., Los Angeles, CA). All samples for total T₄ and total T₃ were run in duplicate and the intra- and interassay variations ranged from 9 to 12%. The lowest calibrator used for hormone analysis was 10 ng/dl and 5 ng/ml for the T₃ and T₄ assays, respectively. The minimum detectable concentration (MDC) for each assay was determined statistically (3 sD above background levels). For all T₃ assays (n = 4), the MDC was 7.8 ng/dl and for all T₄ assays (n = 4), the MDC was 4.9 ng/ml. In cases in which the sample result was below the level of detection, the result was set by default to the MDC for statistical purposes.

Immunohistochemistry

Animals were deeply anesthetized with an overdose of phenobarbital (100 mg/kg, ip) and perfusion fixed through the aorta with 4% paraformaldehyde. The brain was removed after perfusion of the animal and stored in 4% paraformaldehyde for several days before being transferred to cryoprotectant and subsequently sectioned at 50 μm using a vibratome. Every section throughout the hippocampus was saved in five consecutive bins such that each bin contained sections throughout the hippocampus at 200-μm intervals. Immunohistochemical staining was performed on control and experimental tissue using batch processing according to the methods of Goodman and Sloviter (27). Briefly, the sections were washed in Tris buffer (pH 7.6) followed by incubation in 1% hydrogen peroxide to remove endogenous peroxidase activity. Sections were then washed sequentially in Tris followed by Tris A (0.1 M Tris plus 0.1% Triton X-100) and then Tris B (0.1 M Tris, 0.1% Triton X-100, 0.05% BSA). The sections were then incubated in antibody for 48 h at 4 C. Anti-PV antiserum (1:100,000 dilution, monoclonal; Sigma) was used to identify PV-containing neurons. On the second day of processing, the sections were incubated in biotinylated secondary antiserum (horse antimouse, dilution 1:400; Vector Laboratories, Burlingame, CA) followed by avidin-biotin complex (ABC Elite; Vector Laboratories; 1:1000 dilution), and visualized with diaminobenzidine as the chromogen. Stained sections were mounted on glass slides, dehydrated, and coverslipped. A series of sections from a minimum of five animals from each dose group (developmental study, hormone replacement study, adult dosing study) and exposure condition (cross-fostering study) were qualitatively evaluated by an observer blinded to the group designation of each subject. GABA neurons were identified by staining sections from animals in the developmental study with anti-GAD67 antiserum (1:7000 dilution, monoclonal; Chemicon, Temecula, CA). GAD-67-IR neurons were visualized using the methods described above.

Stereological assessment of PV-IR

The density of PV-IR neurons was determined in the hippocampus and somatosensory cortex in coronal sections from PN23 animals using unbiased stereological techniques. In the hippocampus the principal cell

body layers of the dentate gyrus and CA1 and CA3 subregions of the hippocampal formation were outlined, and the cell density was estimated for each region independently. The decrease in PV-IR in the cortex of exposed animals was so severe that we were unable to assess cell density in specific cortical layers. To ensure that the same area of cortex was analyzed for each animal, the right hemisphere of each section was outlined from the cingulate cortex to the rhinal fissure. A minimum of five sections were evaluated for each of five to seven animals/dose group. Cell density was determined using the optical fractionator stereological probe of StereoInvestigator (Microbrightfield, Williston, VT).

The following method was used to quantify the decrease in process staining of PV-IR neurons in the dentate gyrus. Cells were selected for evaluation using the optical fractionator probe (StereoInvestigator) and a 40-by-40-μm frame was placed over each PV-positive cell. A score of 3, indicative of rich process staining, was assigned if processes emanating from the cell touched three or four sides of the frame. Moderate process staining was enumerated by a score of 2 if processes contacted one or two sides of the frame. A score of 1, indicating minimal staining, was assigned if the processes did not expand to touch any wall of the frame. A total of five sections from each of five animals in each dose group was assessed in this manner, resulting in 21–33 cells/section evaluated in the 0 ppm group, four to 19 cells/section in the 3 ppm group, and two to 12 cells/section in the 10 ppm group. Scores were averaged across sections for a given animal and the mean score/animal was subjected to statistical analysis.

Western blot analysis

One animal from each litter was killed by decapitation on PN14, PN21, and PN78, the brain removed, and the hippocampus dissected, frozen on dry ice, and stored at −80 C for later analysis. Tissue was homogenized by brief sonication in ice-cold solubilizing buffer containing 1% Triton X-100, 20 mM Tris (pH 7.5), 150 mM NaCl, 1 mM EDTA, 10% glycerol, 1 mM NaF, 1 mM Na3VO4, and 0.5% protease inhibitors (Protease Inhibitor Cocktail III; Calbiochem, La Jolla, CA). The insoluble material was removed by centrifugation at $10,000 \times g$ for 10 min at 4 C. An aliquot of the supernatant was taken for protein determination, and the remaining supernatant was added to an equal volume of Laemmli's sample buffer (Bio-Rad, Hercules, CA) to give a final protein concentration of 2.0 mg/ml, and samples were boiled at 100 C for 5 min. Samples were resolved by SDS-PAGE on 4–15% Tris-HCl gels (161–1122; Bio-Rad) followed by electrophoretic transfer onto polyvinyl difluoride membranes (162–0218, Bio-Rad). The blots were blocked for 1 h with 5% nonfat dried milk (Bio-Rad) at room temperature and then incubated overnight at 4 C with an antibody specific to PV (AB11427, rabbit polyclonal to rat skeletal muscle PV; Abcam, Cambridge, MA). After three short washes, the blots were incubated for 1 h with 1:10,000 horseradish peroxidase-conjugated goat antirabbit antibody (074–1506; KPL, Gaithersburg, MD). The blots were visualized using a chemiluminescence substrate (34076, SuperSignal West Dura extended duration substrate; Pierce, Rockford, IL), and the light images of the 13.1-kDa band were collected and analyzed photometrically with a Fluor-S MultiImager and Quantity One software (version 4.3.1; Bio-Rad). For all Western blots, two to three lanes on each gel were reserved for molecular weight standards (161–0374, PrecisionPlus dual color; Bio-Rad) and quality control (QC) samples. The QC samples were prepared from a pool of a hippocampi harvested from naïve young adult rats, and aliquots of the pool were maintained at −80 C. One aliquot was used for each gel or series of gels run at one time. After correction for background chemiluminescence, the signals from target bands on a gel were normalized to the average signal for the QC sample bands to simplify comparison across gels and reduce intergel variability. The coefficient of variation for the QC values across gels was typically less than 10%.

Animal surgery

Adult male offspring (4–10 months of age) were anesthetized with urethane (1–2 gm/kg, ip), mounted in a stereotaxic frame and electrodes placed into the perforant path and dorsal dentate gyrus according to standard techniques (see Ref. 14). Briefly, a stimulating electrode (bipolar twisted stainless steel wire, 250 μm in diameter, insulated except for the cut tips, crimped onto gold-plated Amphenol pins) was lowered into the angular bundle of the perforant path according to flat skull

stereotaxic coordinates (7.2 mm posterior to bregma, 4.1 mm lateral to the midline). An insulated monopolar nichrome wire-recording electrode was lowered into the ipsilateral dentate gyrus 3.5 mm posterior to bregma and 2–2.2 mm lateral to the midline. Nominal depths for stimulating and recording electrodes were 2.2 and 3.5 mm below dura, respectively, but optimal depth placement was achieved through electrophysiological monitoring of the response evoked in the dentate gyrus after a single-pulse perforant path stimulation. Stimulation of the perforant path evokes a monosynaptic extracellular field potential that can be reliably recorded from electrodes placed in the hilar region (28, 29). The field potential is comprised of an initial positive component, the excitatory postsynaptic potential and a negative compound action potential, the population spike (PS) (see Fig. 9). The dendritic response provides an index of synaptic activity comprising the summed excitatory postsynaptic potentials. PS amplitude was estimated by calculating the value of the tangent that extends from the lowest value of the negative potential to the point of intersection of a line connecting the positive peaks that mark the beginning and the end of the negative spike potential (29). Two animals were assessed each day, and dose groups were counterbalanced over days to equate the mean age across groups. Data represent 21 0-ppm, 24 3-ppm, and 13 10-ppm animals sampled from 14, 15, and 9 litters, respectively. No more than two animals from any given litter are represented.

Paired pulse depression/facilitation

Once optimal electrode placement based on response morphology and amplitude was achieved, responses evoked by single-pulse stimulation of the perforant path (biphasic square wave pulses, 0.1 msec duration using a Grass S-88 stimulator and PSIU-6 constant current converters) were monitored at 30-min intervals for the next 2 h to ensure stability before commencement of formal testing (30). Responses were amplified, digitized (33 kHz sampling rate), averaged using LabWindows (National Instruments, Austin, TX) and custom designed software, and stored on a personal computer for later analysis. Upon stability of the field potential recording, two pulses (conditioning pulse followed by the test pulse) of equal stimulus intensity were delivered at a variety of interpulse intervals (IPIs = 10, 20, 30, 70, and 250 msec) and stimulus intensity levels. Intensities were chosen to produce PS amplitudes of the first pulse (conditioning pulse) equivalent to 20, 50, and 100% of the maximal population spike amplitude recorded at 1500 μA. Ten pulse pairs were averaged at each IPI and each intensity. Data were expressed as a ratio of test pulse to conditioning pulse PS amplitude and converted to a percent. A value of less than 100% reflects paired pulse depression, a ratio greater than 100%, paired pulse facilitation.

Statistical analyses

Results of cell counts, neuronal process staining, and Western blot analyses were assessed using one-way ANOVA, and where appropriate mean contrast tests were performed using Tukey's *t* test. Cell counts for saline *vs.* T$_4$ groups in the replacement studies were evaluated using a *t* test. Paired-pulse functions were assessed using a three-way repeated-measures ANOVA. Repeated factors included three levels of intensity and five levels of IPI. Step-down ANOVAs and Tukey's mean contrast tests were used in the event of significant two-way (dose × intensity or dose by interval) or three-way (dose × intensity × interval) interactions.

Results

Hormone insufficiency during development and adulthood

Serum thyroid hormone levels for animals in the developmental study were previously reported and are reiterated here to provide a context of the level of hormonal disruption induced by developmental exposures to PTU (5, 16). At weaning, 3 ppm PTU reduced T$_4$ by 70% relative to controls. All animals in the high-dose group fell below the level of detection of the assay. Serum levels of T$_3$ were reduced by 30 and 70%, respectively, in the 3- and 10-ppm dose groups. In the cross-fostering study, hormone analyses for postnatal only or prenatal + postnatal exposure were consistent with

those of the 10-ppm dose group reported in Sui *et al.* (16). PTU-exposed pups cross-fostered to control dams at birth had thyroid hormone levels within the normal range at weaning. Hormone levels of all groups had returned to control values by PN77 (earliest postweaning time sampled) well in advance of adult immunochemical and neurophysiological assessments. Hormone levels in the adult dosing study were also reduced in a dose-dependent manner. One month of exposure to 3 ppm PTU beginning in adulthood resulted in a 78% reduction in serum T_4 concentration from control levels of 48.7 ± 4.46 ng/ml. Serum T_4 in all 10-ppm animals fell below the level of detection of the assay (4.9 ng/ml). Concentrations of T_3 were reduced by 31 and 61% of control values (82.0 ± 8.75 ng/dl) for low- and high-dose groups, respectively.

PV immunohistochemistry is reduced by hormonal insufficiency

Bands of cell body staining with rich expansion of the axonal and dendritic plexuses are characteristic of PV-IR in the neocortex (Fig. 1A). In hippocampus, PV-IR neurons exhibit a striking lamellar distribution with cell bodies concentrated in stratum pyramidale of areas CA1 and CA3 and in the granule cell layer including the subgranular zone of the dentate gyrus. The dendrites and axons of PV-IR neurons within the hippocampus penetrate the dendritic and axonal layers of pyramidal and granule cell body layers (Fig. 1D).

PV-IR was dramatically reduced in the neocortex and hippocampus of PN23 animals exposed to PTU throughout gestation and lactation. Figure 1, A–C, displays representative sections of somatosensory cortex from control and PTU-exposed animals in which a pattern of decreased immunoreactivity is evident in treated animals. Cell body and extensive neuronal process staining present in the cortex of control animals was greatly diminished in low-dose animals (Fig. 1B), and PV-IR of cell bodies and processes was almost completely absent in subjects from the high-dose group (Fig. 1C). Qualitatively, in all cases (five of five 3 ppm and five of five 10 ppm animals), clear differences from control were observed, but a distinction was not always possible between the high- and low-dose groups. Similarly in hippocampus, pyramidal cell layers and the dentate gyrus displayed a diminished pattern of immunoreactivity, with striking reductions in both cellular and neuronal process staining (Fig. 1, D–F).

Estimates of cell number using unbiased stereological methods revealed significant, dose-dependent reductions in the density of PV-immunopositive neurons in neocortex [Fig. 2, F (2,17) = 14.47, P < 0.0002] and all three subregions of the hippocampus [dentate gyrus F (2,13) = 329.28, P < 0.0001; CA1 F (2,13) = 182.6, P < 0001; P < 0.0001; CA3 F (2,13) = 79.12, P < 0.0001]. In cells with a positive PV-IR profile, neuronal process staining was diminished in treated animals in both cortex and hippocampus (see Figs. 1 and 3). Quantification of axonal and dendritic plexus staining was performed for PV-IR cells in the dentate gyrus according to procedures outlined in *Materials and Methods*. Significant dose-dependent reductions were observed in the mean plexus score [F (2,12) = 115.1, P < 0.0001, Fig. 3E] and the percent of cells/animal exhibiting a high degree of neuronal process staining [F (2,12) = 79.56, P < 0.0001, Fig. 3F]. This assessment of neuronal process immunoreactivity was limited to the level of the interneuron cell body and as such underestimates the magnitude of the effect of hormone insufficiency on neuronal process expression (see Fig. 3). Nonetheless, clear dose-dependent reductions were evident as a function of PTU exposure.

Thyroid hormone replacement

Offspring from five 10-ppm exposed litters were administered saline or T_4 on PN8–PN14, the time of peak expression of PV in the forebrain (26). T_4 replacement during this window resulted in a significant increase in the PV-IR on PN27 in both neocortex and hippocampus relative to PTU animals receiving injections of saline (Fig. 4). Quantification of PV-IR neuronal density in the neocortex confirmed our qualitative impressions, revealing a significant augmentation of PV-IR neurons in 10-ppm pups receiving T_4 (mean = 7814 ± 323 cells/mm³) relative to saline (mean = 4901 ± 597 cells/mm³, P < 0.001). The reduction of PV-IR loss by direct supplementation of pups with T_4 indicates that the decrease in PV-IR is thyroid hormone dependent.
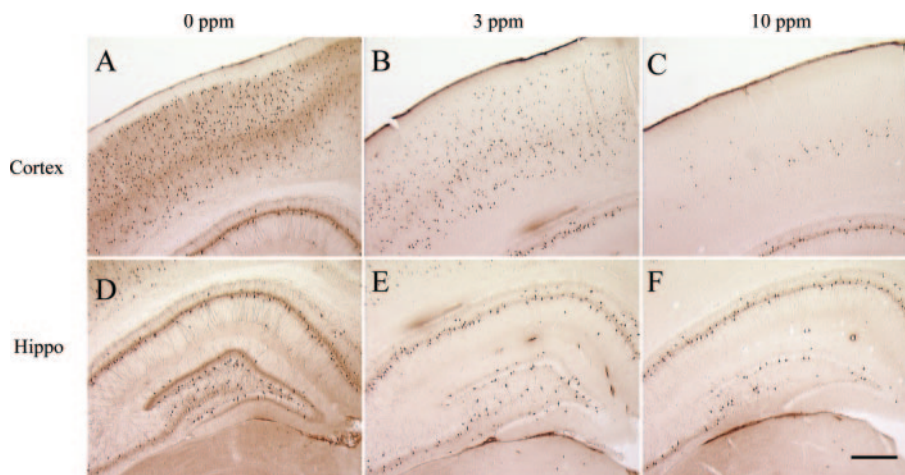

Fig. 1. PV-IR is suppressed in hypothyroid animals before weaning. PV-IR in neocortex (A–C) and hippocampus (Hippo; D–F) is reduced on PN23 in animals exposed perinatally to 3- or 10-ppm PTU. Animals remained on PTU until the time the animals were killed. Clear diminution of PV-IR fiber staining is apparent in neocortex (B) and hippocampus (E) of low-dose animals. At high doses of PTU, cell body in addition to neuronal process staining for PV is severely suppressed (calibration, 500 μM).
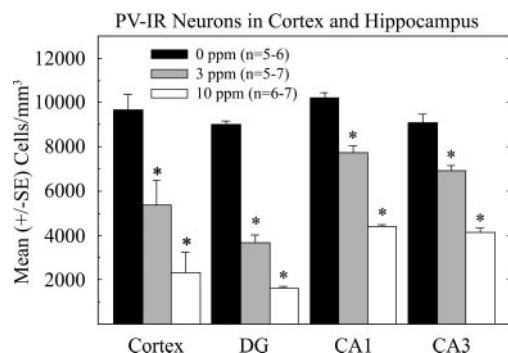
FIG. 2. Cell density of PV-IR cells (mean cells/mm³ ± SE) in cortex and subfields of the hippocampal formation of PTU-exposed animals. In PN23 animals the density of cells expressing PV was dose-dependently reduced in neocortex as a function of PTU exposure. Subregional assessment in hippocampus revealed a similar pattern in area CA1, CA3, and dentate gyrus (DG), and the magnitude of reduction appeared greater in the dentate gyrus than other hippocampal subregions (Tukey's; *, $P < 0.05$).

Cell loss vs. phenotypic expression

It is important to determine whether developmental PTU exposure leads to a lower number of GABA cells in general or simply alters the phenotype of GABAergic interneurons.
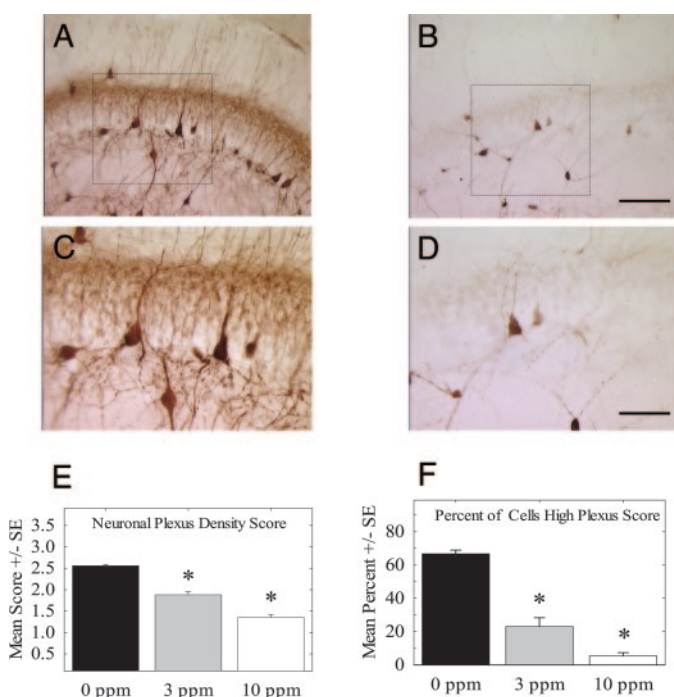

FIG. 3. High magnification of PV-IR neurons in the dentate gyrus from a control (A) and 10-ppm (B) animal demonstrate reduced staining of neuronal processes in PTU-exposed animals on PN23. *Boxed area* is enlarged in C and D. Quantitative estimates of the degree of neuronal process staining were performed as described in *Materials and Methods*. Neuronal plexus staining at the level of the interneuron cell body was rated on a scale of 1–3 (see text), with a score of 3 indicating a rich plexus with multiple processes and a score of 1 indicating few processes were evident. PTU-exposed animals showed a dose-dependent reduction in the mean (±SE) neuronal process score (E) and percent of cells/animal (mean ± SE) with rich plexus staining attaining a high score of 3 (F) (Tukey's; *, $P < 0.05$) (calibration A and B, 250 µM; C and D, 125 µM).

To distinguish between these two possibilities, the GABA-ergic neurons were visualized by immunostaining for glutamic acid decarboxylase (GAD-67), a synthesis enzyme for GABA. Unlike PV, GAD-67 is expressed in the majority of GABA interneurons including those that also express PV (17–20, 22). We did not detect a qualitative difference in GAD immunoreactivity between control (n = 3), 3-ppm (n = 3), and 10-ppm (n = 3) PTU-exposed animals (Fig. 5). This observation, coupled with findings from the hormone replacement experiment, indicates that the decrease in PV-IR resulted from an alteration in phenotypic expression of PV, rather than neuronal loss.

Alterations in PV-IR persist to adulthood

PV-IR remained abnormal in the neocortex and hippocampus of adult offspring of hypothyroid dams (Fig. 6). PTU-induced reductions in cellular and neuronal staining remained in cortex (Fig. 6, A–D) and hippocampus (Fig. 6, E–H), despite a return to euthyroid status. It is apparent from comparisons of Fig. 1 (PN23) and Fig. 6 (PN86) that significant recovery has occurred with age and return to control levels of thyroid hormones. In adulthood, differences between groups were less striking and variability in the degree of staining within a dose group was higher. The variability can be seen in Fig. 6 by comparing cortex (Fig. 6, C and D) and hippocampus (Fig. 6, G and H) from two different animals in the high-dose group. Nonetheless, PV-IR was still clearly suppressed relative to controls in four of five 3-ppm and five of five 10-ppm animals evaluated. These findings indicate that developmental hormone insufficiency produced a permanent alteration in the expression of PV in both of these brain regions.

Western blots performed on hippocampus from littermates killed on PN14, 21, and 78 were consistent with dose-dependent reductions in PV observed immunocytochemically (Fig. 7). Protein levels increased with age in control animals and were dose-dependently suppressed in PTU-treated animals at all time points [PN14 $F_{(2,21)} = 38.44$, $P < 0.0001$; PN21 $F_{(2,24)} = 38.16$, $P < 0.0001$; PN78 $F_{(2,30)} = 3.51$, $P < 0.04$]. As with the immunohistochemistry findings, the effects of thyroid hormone insufficiency appeared more robust at the early time points (PN14 and PN21) when animals were maintained on PTU with some recovery evident by PN78. However, both immunohistochemistry (Fig. 6) and Western blot analyses (Fig. 7) indicate lasting reductions in PV expression in adulthood despite normal thyroid status.

Postnatal hormonal insufficiency is required

A cross-fostering study was performed to determine whether a critical window of hormone insufficiency was necessary to produce alterations in expression of PV. PV-IR in the cortex and the hippocampus of animals deprived of thyroid hormone in the prenatal (Pre) period only [*i.e.* pups born to hormone-deficient dams but fostered to control (Con) dams at birth] did not differ from control pups (Con *vs.* Pre, Fig. 8, A and C, E and G)]. Animals whose hormone deprivation began postnatally (Post) (*i.e.* born to control dams and cross-fostered at birth to PTU-treated dams) showed a pattern of reduced PV-IR in both cortex (Post, Fig. 8B) and

FIG. 4. T_4 replacement between PN8 and PN14 significantly ameliorated the loss of PV-IR in cortex (*top panels*) and hippocampus (Hippo; *bottom panels*) assessed on PN27. Control (A and D). Littermates from 10 ppm PTU group treated with saline (B and E) or 100 μg/kg T_4 (C and F) on PN8–PN14. Cell counts verified conclusions based on qualitative examination for the neocortex (see text). Return of PV-IR with T_4 supplementation indicates that the phenotypic expression of PV is thyroid hormone dependent. ($P < 0.05$, calibration, 500 μM).
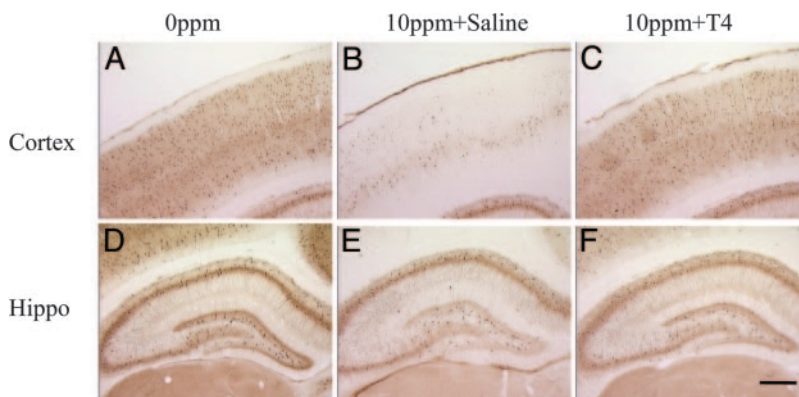
hippocampus (Fig. 8F) relative to control and prenatal-only exposures. However, the diminution of PV-IR in animals experiencing hormone insufficiency restricted to the postnatal period appeared to be less severe than in animals deprived continuously throughout the pre- and postnatal period (PRE+POST, compare Fig. 8B *vs.* 8D and 8F *vs.* 8H). Animals whose exposure to PTU began in adulthood did not appear to show any effect of thyroid hormone insufficiency on PV immunoreactivity (data not shown). Thus, hormone insufficiency *per se* is not the critical determinant of altered PV-IR but rather the developmental window over which it occurs.

Synaptic inhibition

The integrity of synaptic inhibition can be assessed in dentate gyrus field potentials by administering pairs of stimulus pulses at varying interpulse intervals. A triphasic pattern of depression, facilitation, and second period of depression characterizes paired pulse responses in population spike amplitude in the dentate gyrus as the interval between pulses is increased from 10 to 250 msec (see Fig. 9A). Graphically these are expressed as a ratio of the amplitude of the second response relative to the first as depicted for naive animals in Fig. 9B. Paired pulse functions are also intensity dependent, the greatest degree of response suppression occurring at brief interpulse intervals and highest stimulus intensities. Figure 9, A and B, displays the interval and stimulus dependence of field responses in the dentate gyrus and the triphasic paired pulse function typical of naive control animals.

As previously reported, baseline population spike amplitudes were diminished at high doses of PTU (5, 14) such that a full intensity profile for paired pulse functions could not be constructed for four of 13 animals in the 10-ppm dose group. In the remaining high-dose animals, a diminution of early (IPIs 10, 20, 30 msec) and late (IPI 250 msec) paired-pulse depression was observed relative to controls (Fig. 9C). Paired-pulse depression of the low PTU dose group did not differ from controls at maximal stimulus intensities (100% Max, Fig. 9C), but increases over control levels of paired pulse facilitation were seen at 70 msec. This pattern of disinhibition was further accentuated in a dose-dependent manner as stimulus strength was systematically reduced, the lowest intensity (20% Max) yielding the largest effects (Fig. 9E). The 3-ppm dose group exhibited deviations from control levels of depression and facilitation at the lowest stimulus intensity at all but the briefest interval. These findings were confirmed by a significant effect of dose [$F (2,51) = 10.63, P < 0.0001$] and a significant dose × interval × intensity interaction [$F (16,408) = 2.53, P < 0.001$] in the overall ANOVA. Step-down ANOVAs at the lowest stimulus intensity (20%, Fig. 9E) demonstrated significant deviations from control in both 3-ppm [dose $F (1,43) = 10.91, P < 0.0019$; dose × interval interaction $F (4,172) = 2.90, P < 0.0235$] and 10-ppm [dose $F (1,28) = 13.43, P < 0.001$; dose × interval interaction $F (4,112) = 2.85, P < 0.0271$] dose groups.

Discussion

This study demonstrates that immunostaining for PV, a calcium-binding protein selectively expressed in interneurons, was dramatically reduced in neocortex and hippocampus in weanling aged animals, thyroid hormone insufficient at the time of assessment. The acute effects of thyroid hormone insufficiency, however, cannot account for alterations in staining as PV-IR remained suppressed in adult offspring after full recovery of thyroid hormone status. Furthermore, this pattern of diminished PV-IR was thyroid hormone dependent as evidenced by recovery with T_4 replacement during the window of maximal PV expression in forebrain areas. Hormone deprivation beginning in the adult period and continuing for 1 month before the animals were killed was

FIG. 5. GABAergic neurons in the cortex of controls (A) at PN23 as visualized by GAD-67 immunoreactivity were not reduced in PTU-treated animals (B, 3 ppm, and C, 10 ppm). Together with results on thyroid hormone replacement (Fig. 4), these findings indicate that a full complement of GABAergic cells remain in hypothyroid animals, but the phenotypic expression of PV within these cells is altered as a result of developmental thyroid hormone insufficiency (calibration, 250 μM).
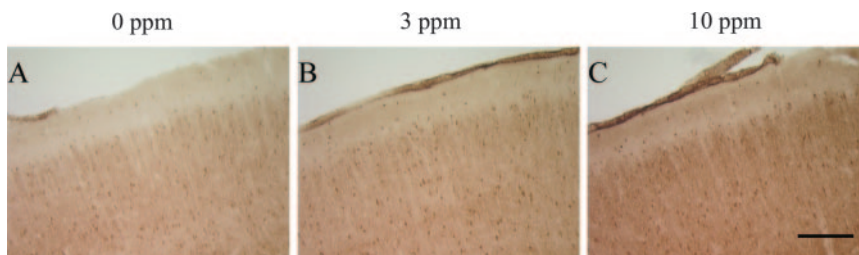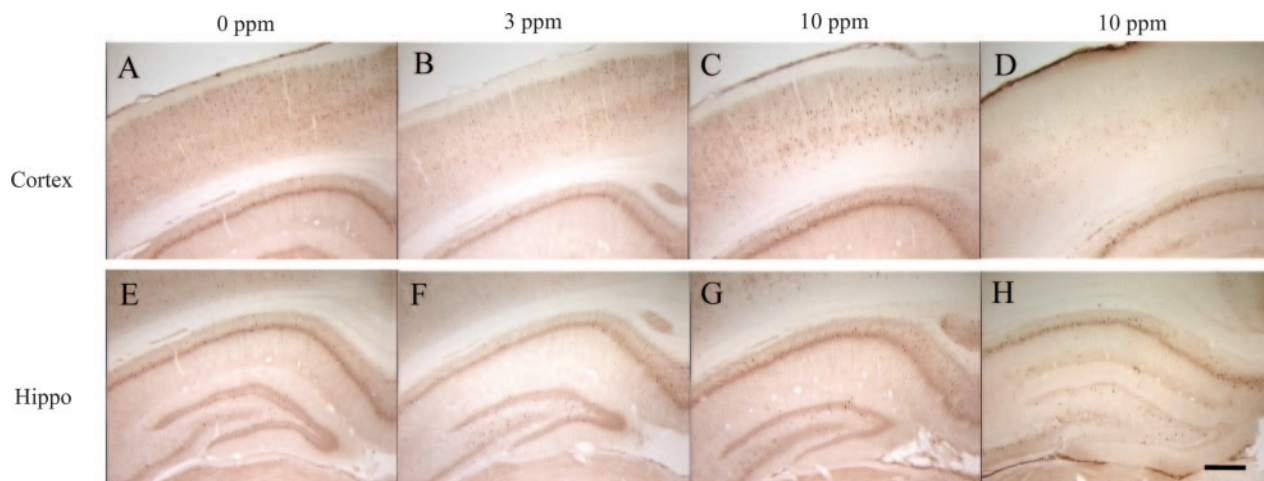
Fig. 6. PV-IR remains suppressed in adult offspring after return to euthyroid state. PV-IR in neocortex (A–D) and hippocampus (Hippo; E–H) remains suppressed in 3- and 10-ppm animals on PN86. Relative to reductions seen on PN23 (Fig. 1), some evidence of recovery is seen, particularly in neuronal process staining in the 3-ppm group (B and F), but significant suppression of PV-IR remains. In these animals, PTU exposure was terminated on PN30 and serum thyroid hormone had returned to control levels at the time the animals were killed. Two examples of 10-ppm animals are shown to demonstrate the range of responsiveness observed within this group. The animal displayed in C and G showed considerably more recovery than the one shown in D and H (calibration, 500 μM).

not accompanied by changes in PV-IR. A persistent change in inhibitory modulation in the dentate gyrus accompanied alterations in PV-IR. Paired-pulse depression was reduced and facilitation enhanced in adult animals developmentally exposed to PTU. The largest differences were found at modest stimulus intensities when presumably inhibitory circuits are not maximally activated and deficiencies more likely to be revealed. Electrophysiological findings of reduced inhibition are consistent with reductions in PV-IR of inhibitory neurons in the dentate gyrus of adult offspring and suggest PTU-induced disinhibition may derive from altered function in this population of interneurons.

Developmental exposure and reduced PV-IR

Neither severe nor continuous hormone deprivation is required to alter PV staining. Significant reductions in PV-IR

Fig. 7. Western blot analysis of the hippocampus revealed dose-dependent reductions in PV at three ages (PN14, PN21, PN78). Data represent mean ($\pm$ SE) normalized chemoluminescence values for the PV band. Although reductions were more robust in younger animals before termination of PTU treatment, adult animals still displayed significant reductions in protein expression despite return to normal hormonal status. (*, Tukey's, $P < 0.05$). *Insets* are representative from immunoblots 0-, 3-, and 10-ppm samples at each age.

were seen in weanling aged animals in the low-dose PTU group exhibiting a moderate level of hormone disruption, and deficiencies in PV-IR were still apparent in adult animals despite return of hormone levels to the normal range. Cell counts performed in the neocortex and hippocampus revealed fewer PV-IR cells in both dose groups relative to controls. There was also a dramatic reduction in PV-IR in the dendritic and axonal processes that normally form the rich fiber plexus surrounding principal cells of cortex and hippocampus. Quantitative assessments were performed on PV-IR cells in the dentate gyrus and verified qualitative impressions of diminished process staining. Results of Western blot analysis were consistent with immunohistochemistry findings, demonstrating a reduction of PV in the hippocampus of treated animals relative to controls. The magnitude of the change in PV assayed by Western blot was less dramatic than that seen immunohistochemically, possibly due to a low signal to noise ratio for PV in hippocampal homogenates.

Our findings are consistent with a previous report of a reduction in the PV neuronal process staining in neocortex of adult rats deprived of hormone in late gestation and remaining thyroid deficient throughout life. Berbel *et al.* (24) demonstrated a diminution of PV-IR in axonal and dendritic processes in inhibitory neurons of the sensory cortex with no change in the number of cells expressing PV. The present study expands on these observations and provides evidence that PV-IR in the hippocampus is also sensitive to developmental thyroid hormone insufficiency. The present findings differ from those of Berbel *et al.* (24), in that PV-IR of the cell soma as well as the intensity of process staining were markedly reduced. However, thyroid hormone replacement effectively reversed the PTU-induced decrease in PV-IR, demonstrating that the PV-IR inhibitory neurons were still present; they had just stopped making PV in the absence of thyroid hormone. Furthermore, results of immunostaining for a marker of GABA neurons indicate, as Berbel *et al.* (24)
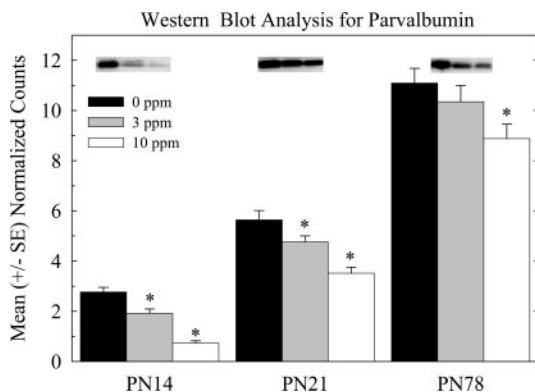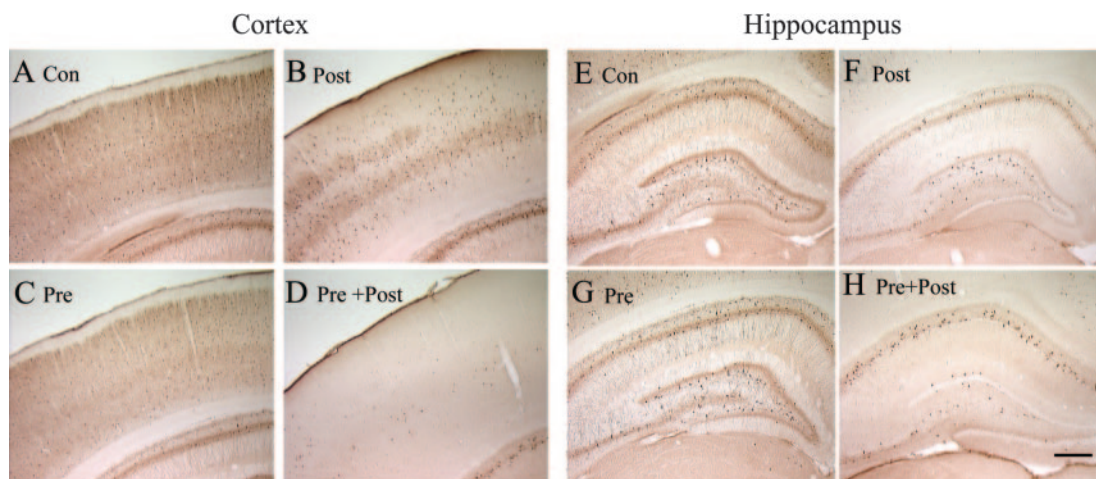
Cortex   Hippocampus

FIG. 8. Postnatal thyroid hormone insufficiency is necessary for altered PV-IR in neocortex (A–D) and hippocampus (E–H). A cross-fostering experimental design revealed that PV-IR was suppressed on PN23 in the neocortex and hippocampus of animals exposed to PTU (10 ppm) beginning in the immediate postnatal period (B and F). More severe reductions in PV-IR were evident in animals exposed throughout gestation and lactation (D and H). No difference from control (A and E) could be detected in the prenatal only exposure group (C and G) (calibration, 500 μM).

concluded, that the total complement of GABA-containing neurons remains intact in hypothyroid animals. Colocalization of PV with GABA ascribes specific electrical and metabolic characteristics to this population of interneurons (18, 20–22). The functional parameters conferred upon interneurons by PV in its capacity to bind calcium may be altered by its absence and ultimately be reflected as disruptions in synaptic inhibition as described below.

The cross-fostering study revealed that hormone insufficiency in the early postnatal period is both necessary and sufficient for altered expression of PV-IR in inhibitory neurons. Hormone reductions restricted to the prenatal period or initiated in adulthood were without effect on PV-IR. However, hormone insufficiency that spanned the prenatal and postnatal period produced more profound deficits in PV-IR that postnatal exposure alone. Severe hormone restrictions in the high dose group that spanned the early prenatal and postnatal period also reduced the numerical density of PV-expressing cells in neocortex and hippocampus (Figs. 1, 2, and 8). Of the three hippocampal subregions, the dentate gyrus appeared to be the most severely impacted (Figs. 2 and 8).

Paired-pulse function as an index of synaptic inhibition

In the dentate gyrus, paired pulses delivered at increasing stimulus intervals produces a triphasic function of depression, facilitation, and a second period of depression. The triphasic pattern results from the influence of temporally successive and overlapping phenomena including a recurrent inhibition, presynaptic facilitation, and a feed-forward inhibition (29). GABA-mediated inhibition by PV-expressing interneurons contributes to varying degrees to each of these phases. Depression of the population spike at very short intervals (early paired pulse depression) is mediated by GABAergic interneurons synapsing on the soma of granule cells and limiting the degree of granule cell firing through feedback circuits (19–23, 29, 31–33). As the interval between pulses is increased, this strong inhibition wanes and paired

pulse facilitation predominates (IPIs of 50–70 msec). Facilitation is the summed effect of presynaptic factors at the granule cell synapse and the interneuron (32, 34–37). A second period of depression following at longer interpulse intervals (250 msec) is smaller in amplitude than that seen at brief intervals and, unlike early paired pulse depression, is reduced in magnitude at maximal stimulus strengths. The mechanism underlying this late-phase inhibition is less well understood but involves feed-forward inhibitory circuits and can be modulated by antagonists of *n*-methyl-*d*-aspartate glutamate receptor (38, 39). We used this *in vivo* field potential analysis to assess integrity of GABA-mediated synaptic transmission in adult offspring after perinatal thyroid hormone insufficiency.

PV-IR and synaptic inhibition

All phases of inhibition were disrupted to varying degrees in animals exposed to PTU and a general pattern of disinhibition was apparent. These effects exhibited a clear dose dependency and were most prevalent at lower stimulus strengths and brief intervals where inhibition is most robust. Animals from the high-dose group displayed reduced levels of inhibition at high stimulus intensities and facilitation rather than depression at modest stimulus strengths. Animals from the low-dose group did not differ from controls at maximal intensities but showed a tendency toward reduced inhibition at the lowest stimulus strength evaluated.

With one exception the pattern of PTU exposure on paired-pulse functions revealed a dose-dependent upward shift to more positive ratios indicative of reduced inhibitory tone or disinhibition. The exception occurs at the 70-msec interval in which a comparable degree of paired pulse facilitation is seen between control and high-dose animals (Fig. 9, D and E). The low-dose group exhibits significant augmentations over control levels of facilitation at 70 msec at all stimulus intensities. This interval of 70 msec corresponds to time when increases in presynaptic transmitter release contribute maximally to the amplitude of the field potential amplitude generated by
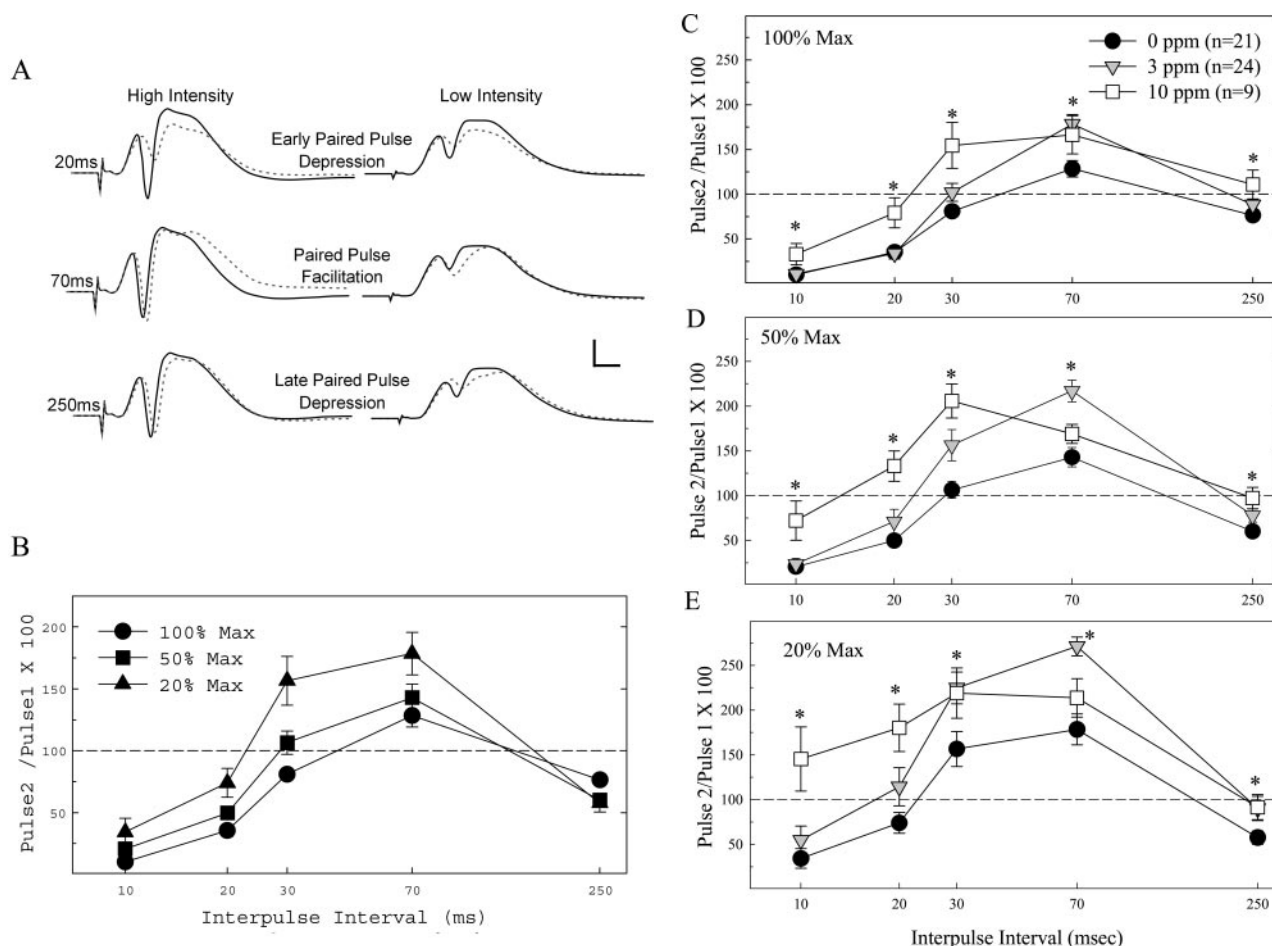
Fig. 9. A, Paired-pulse functions in dentate gyrus of naive control animals are triphasic and intensity dependent. Overlaid waveforms delivered at brief intervals (20 msec, *top*) show suppression of the population spike of the second pulse of the pair (*broken line*) relative to the first (*solid line*) at maximal stimulus strength (*left*) that is lessened as stimulus intensity is reduced (*right*). Delaying the second pulse by 70 msec produces facilitation of the second response relative to the first (*middle*). At the longest interval tested (250 msec), modest inhibition is evident at low stimulus intensities (*right*) but is reduced at maximal stimulus strength (*left*) (calibration 2 msec, 5 mV). B, Expressing the relationship of population spike amplitude as a percent of second-response amplitude relative to the first (pulse 2/pulse 1 × 100) produces a triphasic curve of depression (percent < 100), facilitation (percent > 100), and depression (percent < 100). Stimulus dependence is shown as an upward shift in the triphasic function with decreasing stimulus strengths (100%–20% Max). C–E, Developmental PTU exposure produces disinhibition in dentate gyrus. A dose-dependent reduction in inhibitory tone was observed in adult animals exposed to PTU from early gestation until weaning. Stimulus intensities were selected to produce maximal (C, 100%) and submaximal (D, 50%, and E, 20% of maximal) population spike amplitudes. High-dose animals exhibited a greater reduction in paired-pulse suppression (mean ± SE) at all intervals and all intensities relative to the 3-ppm dose group, and effects were largest at the lowest stimulus intensity (E). However, paired-pulse facilitation at 70 msec was not distinct from control values at 20 and 50% stimulus intensities in the high-dose group (D and E) but was significantly increased in the low-dose group. Impairments in presynaptic release mechanisms in addition to altered inhibitory function may underlie this pattern in high-dose animals (see text; *, Tukey's, $P < 0.05$).

the second pulse of the pair (24, 33, 36, 39, 40). Decrements in facilitation in the high dose relative to the low-dose group may reflect an independent reduction in the processes that control presynaptic transmitter release that summate and outweigh reductions in GABA-mediated inhibition at high doses of PTU. Deficits in presynaptic transmitter release as measured using paired pulse techniques have been previously reported for excitatory postsynaptic potentials in area CA1 of hippocampal slices derived from hypothyroid animals (12, 13, 16).

Our data clearly demonstrate that thyroid hormone insufficiency correlates with a decrease in PV-IR in the hippocampus and reduced inhibitory function in the dentate gyrus. The absence of PV in soma and dendrites of inter-

neurons may affect the firing properties of these cells and alter the network response to excitatory neurotransmission. The extensive loss of the PV-IR neuronal plexus in the hippocampus raises the question of whether the cell processes and the synaptic contacts they make are absent or simply failing to express PV. In a TRα1 mutant mouse model, altered PV-IR could be reversed in adulthood with exogenous administration of a high dose of T_3 (25). In the present study, T_4 replacement during the peak period of PV expression provided significant protection against loss of PV-IR. However, full recovery did not occur after termination of PTU treatment and return of thyroid hormones to control levels in adult offspring. Reduced PV expression in adult offspring of hormone insufficient dams was also accompanied by im-

paired inhibitory function. Altered PV-IR has been associated with seizure activity in hippocampus in some epilepsy models (41), and enhanced seizure susceptibility has been reported in hypothyroid animals (4, 42, 43). Disinhibition may also contribute to paradoxical increases in long-term potentiation of the population spike previously reported in dentate gyrus and area CA1 after developmental thyroid hormone insufficiency (5, 14–16).

In summary, we have identified perturbations in the expression of a protein selectively expressed in interneurons of the hippocampus and cortex and correlated these anatomical aberrations with deficits in synaptic function. Thyroid hormone insufficiency in the early postnatal period is critical for the alteration in PV expression, and only modest and transient periods of hormone insufficiency are required to induce permanent changes in anatomical and functional indices. Although excitatory glutamatergic neurons far outnumber inhibitory GABAergic neurons in the forebrain, their expansive dendritic trees and rich synaptic plexus account for 30–40% of all cortical synapses (44). As such, the functional consequence of even a minor shift in the balance of excitation and inhibition can be profound. Disruption in the genesis, migration, and synaptic connectivity of interneurons has been linked to a number of developmental and psychiatric disorders including childhood epilepsy, autism and schizophrenia (45). We propose that altered protein expression in interneurons in dentate gyrus may underlie some of the impairments in synaptic plasticity and cognition characteristic of thyroid hormone insufficiency during development.

Acknowledgments

References

1. **Anderson, GW, Schoonover, CM, Jones, SA** 2003 Control of thyroid hormone action in the developing rat brain. Thyroid 13:1039–1056
2. **Bernal J, Guadano-Ferraz A, Morte B** 2003 Perspectives in the study of thyroid hormone action on brain development and function. Thyroid 13:1005–1012
3. **Bernal J** 2002 Action of thyroid hormone in brain. J Endocrinol Invest 25:268–288
4. **Auso E, Lavado-Autric R, Cuevas E, Del Rey FE, Morreale De Escobar G, Berbel P** 2004 A moderate and transient deficiency of maternal thyroid function at the beginning of fetal neocorticogenesis alters neuronal migration. Endocrinology 145:4037–4047
5. **Gilbert ME, Sui L** 2006 Dose-dependent reductions in spatial learning and synaptic function in the dentate gyrus of adult rats following developmental thyroid hormone insufficiency. Brain Res 1069:10–22
6. **Lavado-Autric R, Auso E, Garcia-Velasco JV, Arufe Mdel C, Escobar del Rey F, Berbel P, Morreale de Escobar G** 2003 Early maternal hypothyroxinemia alters histogenesis and cerebral cortex cytoarchitecture of the progeny. J Clin Invest 111:1073–1082
7. **Morreale de Escobar G, Obregon MJ, Escobar del Rey F** 2004 Role of thyroid hormone during early brain development. Eur J Endocrinol 151(Suppl 3):U25–U37
8. **Forrest D** 2004 The developing brain and maternal thyroid hormone: finding the links. Endocrinology 145:4034–4036
9. **Guadano Ferraz A, Benavides Piccione R, Venero C, Lancha C, Vennstrom B, Sandi C, DeFelipe J, Bernal J** 2003 Lack of thyroid hormone receptor α1 is associated with selective alterations in behavior and hippocampal circuits. Mol Psychiatry 8:30–38
10. **Dong J, Yin H, Liu W, Wang P, Jiang Y, Chen J** 2005 Congenital iodine deficiency and hypothyroidism impair LTP and decrease C-fos and C-jun expression in rat hippocampus. Neurotoxicology 26:417–426
11. **Niemi WD, Slivinski K, Audi J, Rej R, Carpenter DO** 1996 Propylthiouracil treatment reduces long-term potentiation in area CA1 of neonatal rat hippocampus. Neurosci Lett 210:127–129
12. **Sui L, Gilbert ME** 2003 Pre- and postnatal propylthiouracil (PTU)-induced hypothyroidism impairs synaptic transmission and plasticity in area CA1 of the neonatal rat hippocampus. Endocrinology 144:4195–4203
13. **Vara H, Martinez B, Santos A, Colino A** 2002 Thyroid hormone regulates neurotransmitter release in neonatal rat hippocampus. Neuroscience 110:19–28
14. **Gilbert ME, Paczkowski C** 2003 Propylthiouracil (PTU)-induced hypothyroidism in the developing rat brain impairs synaptic transmission and plasticity in the dentate gyrus of the adult hippocampus. Dev Brain Res 145:19–29
15. **Gilbert ME** 2004 Alterations in synaptic transmission and plasticity in area CA1 of adult hippocampus following developmental hypothyroidism. Dev Brain Res 148:11–18
16. **Sui L, Anderson WA, Gilbert ME** 2005 Impairment in short-term but enhanced long-term synaptic potentiation and ERK activation in adult hippocampal area CA1 following developmental thyroid hormone insufficiency. Toxicol Sci 85:647–656
17. **Celio MR** 1986 Parvalbumin in most γ-aminobutyric acid-containing neurons of the rat cerebral cortex. Science 231:995–997
18. **Fukuda T, Heizmann CW, Kosaka T** 1997 Quantitative analysis of GAD65 and GAD67 immunoreactivities in somata of GABAergic neurons in the mouse hippocampus proper (CA1 and CA3 regions), with special reference to parvalbumin-containing neurons. Brain Res 764:237–243
19. **Fukuda T, Aika Y, Heizmann CW, Kosaka T** 1996 Dense GABAergic input on somata of parvalbumin-immunoreactive GABAergic neurons in the hippocampus of the mouse. Neurosci Res 26:181–194
20. **Katsumaru H, Kosaka T, Heizmann CW, Hama K** 1988 Immunocytochemical study of GABAergic neurons containing the calcium-binding protein parvalbumin in the rat hippocampus. Exp Brain Res 72:347–362
21. **Kawaguchi Y, Katsumaru H, Kosaka T, Heizmann CW, Hama K** 1987 Fast spiking cells in rat hippocampus (CA1 region) contain the calcium-binding protein parvalbumin. Brain Res 416:369–374
22. **Kosaka T, Katsumaru H, Hama K, Wu JY, Heizmann, CW** 1987 GABAergic neurons containing the Ca2+-binding protein parvalbumin in the rat hippocampus and dentate gyrus. Brain Res 419:119–130
23. **Knowles WD, Schwartzkroin PA** 1981 Local circuit synaptic interactions in hippocampal brain slices. J Neurosci 1:318–322
24. **Berbel P, Marco P, Cerezo JR, DeFelipe J** 1996 Distribution of parvalbumin immunoreactivity in the neocortex of hypothyroid adult rats. Neurosci Lett 204:65–68
25. **Venero C, Guadano-Ferraz A, Herrero AI, Nordstrom K, Manzano J, de Escobar, GM, Bernal J, Vennstrom B** 2005 Anxiety, memory impairment, and locomotor dysfunction caused by a mutant thyroid hormone receptor α1 can be ameliorated by T3 treatment. Genes Dev 19:2152–2163
26. **Solbach S, Celio MR** 1991 Ontogeny of the calcium binding protein parvalbumin in the rat nervous system. Anat Embryol 184:103–124
27. **Goodman JH, Sloviter RS** 1993 Cocaine neurotoxicity and altered neuropeptide Y immunoreactivity in the rat hippocampus; a silver degeneration and immunocytochemical study. Brain Res 616:263–272
28. **Lomo T** 1971 Patterns of activation in a monosynaptic cortical pathway: the perforant path to the dentate area of the hippocampal formation. Exp Brain Res 12:18–45
29. **Gilbert, ME, Burdette LJ** 1995 Hippocampal field potentials: a model system to characterize neurotoxicity. In: Chang LW, Slikker W, eds. Neurotoxicology: approaches and methods. New York: Academic Press; 183–204
30. **Gilbert ME, Mack, CM** 1999 Field potential recordings in dentate gyrus of urethane anesthetized rats: stability of baseline. Hippocampus 9:277–287
31. **Burdette LJ, Gilbert ME** 1995 Stimulus parameters affecting paired pulse depression of dentate gyrus granule cell field potentials: I. Stimulus intensity. Brain Res 680:53–62
32. **Papatheodoropoulos C, Kostopoulos G** 1998 Development of a transient increase in recurrent inhibition and paired-pulse facilitation in hippocampal CA1 region. Dev Brain Res 108:273–285
33. **Tuff LP, Racine RJ, Adamec R** 1983 The effects of kindling on GABA-mediated inhibition in the dentate gyrus of the rat. I. Paired pulse depression. Brain Res 277:79–90

34. **Brucatto FH, Morrisett RA, Wilson WA, Swartzwelder HS** 1992 The GABAB antagonist, CGP-35348, inhibits paired pulse disinhibition in the rat dentate gyrus *in vivo*. Brain Research 588:150–153

35. **Canning, KJ and Leung, LS** 2000 Excitability of rat dentate granule cells in vivo is controlled by tonic and evoked GABAB receptor-mediated inhibition. Brain Res 863:271–275

36. **Fisher SA, Fischer TM, Carew CJ** 1997 Multiple overlapping processes underlying short-term synaptic enhancement. Trends Neurosci 20:170–177

37. **Zucker RS** 1989 Short-term synaptic plasticity. Annu Rev Neurosci 12:13–31

38. **Gilbert ME, Burdette LJ** 1996 Enhancement of paired pulse depression in the dentate gyrus *in vivo* by the NMDA antagonist, MK-801 and electrical kindling. Brain Res 732:201–208

39. **Joy RM, Albertson TE** 1993 NMDA receptors have a dominant role in population spike paired pulse facilitation in the dentate gyrus of urethane-anesthetized rats. Brain Res 604:273–282

40. **Steffensen SC, Henriksen SJ** 1991 Effects of baclofen and bicuculline on inhibition in the fascia dentata and hippocampus regio superior. Brain Res 538:46–53

41. **Scotti AL, Kalt G, Bollag O, Nitsch C** 1997 Parvalbumin disappears from GABAergic CA1 neurons of the gerbil hippocampus with seizure onset while its presence persists in the perforant path. Brain Res 760:109–117

42. **Meisami E, Valcana T, Timiras PS** 1970 Effects of neonatal hypothyroidism on the development of brain excitability in the rat. Neuroendocrinology 6:160–167

43. **Pacheco-Rosado J, Hernandez-Garcia A, Ortiz-Butron R** 2004 Perinatal hypothyroidism increases the susceptibility to lidocaine-kindling in adult rats. Neurosci Lett 367:186–188

44. **Krieger DT** 1983 Brain peptides: what, where and why? Science 222:975–985

45. **Levitt P, Eagleson KL, Powell EM** 2004 Regulation of neocortical interneuron development and the implications for neurodevelopmental disorders. Trends Neurosci 27:400–406

Endocrinology **is published monthly by The Endocrine Society (http://www.endo-society.org), the foremost professional society serving the endocrine community.**

Erratum

In the article "Testicular Edema Is Associated with Spermatogonial Arrest in Irradiated Rats" by Karen L. Porter, Gunapala Shetty, and Marvin L. Meistrich (*Endocrinology* **147:**1297–1305), the authors note that the units for Fluid Volume in Fig. 4A should be ml (milliliters) not μl (microliters). *The authors regret the error and apologize for any problems that this may have caused.*